Journal of Engineering Science and Technology
Special Issue on SOMCHE 2014 & RSCE 2014 Conference, January (2015) 68 - 78


# A CFD STUDY OF A PARTIAL COMBUSTION LANCE

WOON PHUI LAW[1], JOLIUS GIMBUN[1,2,*]

[1]Faculty of Chemical and Natural Resources Engineering, Universiti Malaysia Pahang, 26300, Gambang, Pahang, Malaysia.
[2]Centre of Excellence for Advanced Research in Fluid Flow (CARIFF), Universiti Malaysia Pahang, 26300, Gambang, Pahang, Malaysia
*Corresponding Author: jolius@ump.edu.my

**Abstract**

A computational fluid dynamics (CFD) simulation of a partial combustion lance (PCL) was presented. The major aim of this paper is to evaluate the influence of oxygen flowrate on its performance. Firstly, a modelling strategy was developed by comparing discretisation schemes, pressure interpolation schemes and Reynolds-averaged Navier-Stokes (RANS) based turbulence models. Three RANS based models were chosen in this work, namely, standard $k$-$\varepsilon$ (SKE), realisable $k$-$\varepsilon$ (RKE) and renormalised (RNG) $k$-$\varepsilon$. Convection and radiation were considered in the heat transfer modelling, whereas combustion was modelled using finite rate-eddy dissipation model. The finding suggested that second-order scheme, standard pressure scheme and SKE provide the best prediction, yielding an error of 5.86% from the experimentally measured temperature. It was found that 40% increase in oxygen flowrate increased the peak combustion temperature of the PCL by about 12%. Dual lance was found to be more effective than the single lance operating at a similar flowrate. Results from this work suggests that the performance of a PCL is significantly depends on the operating condition. CFD tool is useful to improve the performance of a combustion system.

Keywords: CFD, Modelling strategy, RANS, Turbulence, Combustion, Oxygen lance

## 1. Introduction

Partial combustion system is often used in iron making plant to increase the reducing gas temperature and to promote in-situ reforming. Installation of a partial combustion system on the transfer line between the reducing gas heater and the iron reduction reactor is vital to reduce the reforming gas consumption and to increase overall reactor performance by increasing its operating temperature. The performance of the PCL may affect the quality of the product.

**Nomenclatures**

| | |
|---|---|
| $C_\mu$ | Coefficient of turbulent viscosity |
| $CH_4$ | Methane |
| CO | Carbon monoxide |
| $CO_2$ | Carbon dioxide |
| $H_2$ | Hydrogen |
| $H_2O$ | Water |
| $h$ | Convective heat transfer coefficient, W/(m$^2$K) |
| $k$ | Turbulent kinetic energy, m$^2$/s$^2$ |
| $N_2$ | Nitrogen |
| $O_2$ | Oxygen |
| $Pr_t$ | Turbulent Prandtl number |
| $Q_C$ | Convective heat transfer rate, W/m$^2$ |
| $Q_R$ | Radiation heat transfer rate, W/m$^2$ |
| $R_\varepsilon$ | Additional rate in RNG $k$-$\varepsilon$ |
| $T_g$ | Gas temperature, K |
| $T_r$ | Radiation temperature, K |
| $T_s$ | Wall surface temperature, K |
| $u$ | Axial velocity, m/s |

***Greek Symbols***

| | |
|---|---|
| $\varepsilon$ | Turbulent dissipation rate, m$^2$/s$^3$ |
| $\varepsilon$ | Emissivity of PCL wall |
| $\rho$ | Density, kg/m$^3$ |
| $\sigma$ | Stefan-Boltzmann constant, 5.67 x 10$^{-8}$ W/(m$^2$K$^4$) |

**Abbreviations**

| | |
|---|---|
| CCD | Charged-coupled device |
| CFD | Computational fluid dynamics |
| EDM | Eddy dissipation model |
| PCL | Partial combustion lance |
| PIV | Particle image velocimetry |
| PRESTO | Pressure staggering option |
| QUICK | Quadratic upwind interpolation for convective kinematic |
| RANS | Reynolds-averaged Navier-Stokes |
| RKE | Realisable $k$-$\varepsilon$ |
| RNG | Renormalised $k$-$\varepsilon$ |
| SKE | Standard $k$-$\varepsilon$ |

The performance of a PCL is affected by several factors such as its operating condition. For instance, low oxygen concentration in combustion air gives a slower combustion rate and smaller flame. This results in insufficiently high combustion temperature and increased pollutant emission [1]. Earlier, Amirshaghaghi et al. [2] reported a decrease in methane gas conversion and lower outlet temperature due to insufficient oxygen supply to the combustion process. Hence, the effect of oxygen flowrate to PCL outlet temperature is studied in this work.

Fluid flow in PCL had been studied extensively both experimentally and numerically [2-5]. A cheaper measurement technique may be performed using a hot-wire anemometry [6]. Advanced techniques such as particle image velocimetry (PIV) can provide detailed visualisations on the flow pattern [7]. However, experimental measurement using PIV is costly and has an inherent limitation. PIV measurement relies on the charge-coupled device (CCD) camera to capture image, hence it is not applicable to an opaque wall, besides it is potentially dangerous to use a PIV for a large industrial-scale PCL operating at a temperature above 1000 K. Moreover, the partial combustion of reducing gas involves turbulence flow, chemical reaction, mass and heat transfer concurrently. Thus, it is difficult to measure and analyse these complex phenomena experimentally. Alternatively, CFD can provide comprehensive information on the complex phenomena in PCL.

The $k$-$\varepsilon$ based turbulence models [2, 8-10], (i.e., SKE, RKE and RNG $k$-$\varepsilon$) are often used due to its low computational effort, robustness and ease to achieve a converged solution. Most of the previous work used the SKE approach without comparing with other turbulence models. In some cases, numerical predictions are not validated with the experimental data [11]. A limited study on the effect of modelling strategy on the prediction accuracy for PCLs is available in the literature. Hence, this work aims to compare various numerical models since it may affect the accuracy of the CFD prediction. A modelling strategy was developed by comparing three different grids, three discretisation methods, four pressure interpolation schemes and three RANS turbulence models. The validation was performed by comparing the predicted temperature with the experimentally measured temperature from our previous work [12]. Once validation was done, the model was used to study the effect of oxygen flowrate on the temperature profile in the PCL.

## 2. CFD Approach

### 2.1. Geometry and computational grid

The geometry of PCL used in this work is similar to the one studied by Zain et al. [12]. A cylindrical PCL consists of two oxygen lances was created and meshed using GAMBIT 2.4.6 as shown in Fig. 1. The cylindrical PCL has a diameter of 1.266 m and measured 6.35 m long. The oxygen lance is installed 1.35 m from the PCL inlet has a length of 0.483 m and a diameter of 0.06 m, while the nozzle has a length of 0.03 m and a diameter of 0.022 m. The inlet temperature of fuel gas is 1203 K and the inlet velocity is 118 m/s. Pure oxygen at 300 K is introduced into PCL through nozzles with 70 m/s of velocity. Figure 2 shows the surface mesh of the PCL. Finer tetrahedral grid was used to mesh the region close to the oxygen lances and nozzles where the combustion occurs. The rest of the PCL domain was meshed using a coarser hexahedral grid. These unstructured meshes were then converted into a polyhedral mesh to enable a higher order discretisation.

### 2.2. Turbulence modelling

Selection of the turbulence model is very important in CFD simulation to obtain a good prediction. In this work, three turbulence models (i.e., SKE, RKE and RNG $k$-$\varepsilon$) was employed. Two-equation SKE is the most-used turbulence model owing

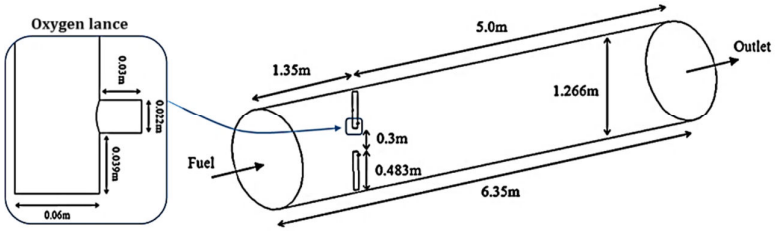


**Fig. 1. A Schematic of a Three-dimensional PCL Geometry.**

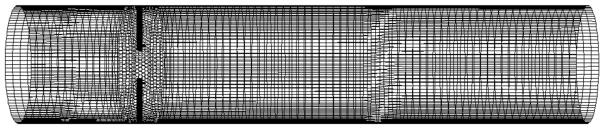

**Fig. 2. Surface mesh of a PCL geometry.**

to its economic, simplicity and robustness. As the shortcoming of SKE is known, an effort was made to introduce a turbulence model that takes into account the swirling effect as well as to ensure a realistic value (non-negative) for $C_\mu$ in $k$-equation [13]. Unlike the SKE, $C_\mu$ coefficient in RKE is not constant and computed as a function of local states of the flow to ensure normal stresses are positive under all flow conditions. Therefore, this model can provide a better prediction on rotation and separation flows [14].

RNG $k$-$\varepsilon$ was derived from renormalised group theory by Yakhot and Orzag [15]. In RNG $k$-$\varepsilon$, the small-scale eddies are eliminated and the transport coefficient is renormalised. RNG differs from SKE because it has an analytical equation for turbulent Prandtl number ($\mathrm{Pr}_t$) and an additional term ($R_\varepsilon$) in $\varepsilon$ transport equation to account for the interaction between turbulence dissipation and mean shear. This additional term gives a slight reduction of dissipation rate, as the result reduces the effective viscosity. Thereby, RNG $k$-$\varepsilon$ model can provide better prediction for a region with large strain rate and streamline curvature [15].

## 2.3. Heat transfer modelling

Radiation and convection are the dominant heat transfer mechanisms in a PCL [16]. In a conventional combustion process, radiation accounts for 96% of total heat transfer while the rest is convection [11]. The convective heat transfer is given by [17];

$$\dot{Q}_C = h\left(T_g - T_s\right) \tag{1}$$

where $h$ is convective heat transfer coefficient, $T_g$ and $T_s$ are temperature of gas and wall surface, respectively. The radiative heat transfer [17] is given by;

$$\dot{Q}_R = \varepsilon\sigma (T_r^4 - T_s^4) \quad (2)$$

where $\varepsilon$ is emissivity of PCL wall, $\sigma$ is the Stefan-Boltzmann constant, $T_r$ is radiation temperature and $T_s$ is the PCL wall surface temperature.

## 2.4. Species Transport Modelling

PCL mainly involves chemical reaction and turbulent mixing. The combustion temperature of PCL is significantly affected by the reaction between the species. In this work, the partial combustion was modelled as follows;

$$CH_4 + 2O_2 \rightarrow CO_2 + 2H_2O \quad (3)$$

$$CH_4 + 1.5O_2 \rightarrow CO + 2H_2O \quad (4)$$

$$CO + 0.5O_2 \rightarrow CO_2 \quad (5)$$

$$H_2 + 0.5O_2 \rightarrow H_2O \quad (6)$$

$$CO_2 \rightarrow CO + 0.5O_2 \quad (7)$$

The oxidation of methane, carbon monoxide and hydrogen in Eqs. (3) to (6) are exothermic, while the carbon dioxide dissociation in Eq. (7) is endothermic. The composition of the inlet gas is given in Table 1. A combination of finite rate and EDM was used to calculate the partial combustion of syngas. In the finite rate model, the chemical reaction is assumed as a slow process while, the turbulent flow is an instantaneous process. Thus, the Arrhenius equation is used to calculate the rate of chemical reaction, whereas the turbulence mixing effect is neglected. In contrast, the chemical reaction rate is controlled by the turbulent mixing in EDM. In the finite rate-EDM approach, both chemical reaction and mixing rate is taken into account whereby the lower rate from either model dictates the reaction.

**Table 1. Composition of the inlet gas.**

| Component | Mass fraction |
|---|---|
| **$CH_4$** | 0.132 |
| **CO** | 0.486 |
| **$CO_2$** | 0.072 |
| **$H_2$** | 0.154 |
| **$H_2O$** | 0.029 |
| **$N_2$** | 0.126 |

## 2.5. Modelling Strategy

The simulation was initialized using a 90 m/s of *x*-velocity and temperature of 1000 K to facilitate faster convergence, since the inlet temperature and *x*-velocity is 1203 K and 118 m/s, respectively. The simulation was performed using a steady-state solver to minimise the complexity and computational effort [11]. The physical properties of fluid (i.e., density, specific heat, thermal conductivity and viscosity) were introduced to the PCL simulation as a piecewise-linear function [18-20]. Initially, the simulation was performed using a first-order discretisation,

but changed to a higher-order discretisation (i.e., second-order and QUICK (Quadratic upwind interpolation for convective kinematic)) once the initial solution is converged. All residuals were set to fall below $1\times10^{-5}$ to ensure a good convergence was achieved. The CFD prediction was recorded for over 1000 iterations and averaged after a convergence. The PCL simulation in this work was performed using a HP Z220 workstation with a quad core processor (Xeon 3.2 GHz E3-1225) and eight Gigabytes of RAM.

## 3. Results and Discussion

### 3.1. Grid dependency analysis

The computational grid may affect the accuracy of CFD prediction, hence a grid dependency analysis was performed to obtain a suitable grid for this work. Three different grid densities of PCL, denoted as coarse (149k nodes), intermediate (418k nodes) and fine grids (694k nodes) were prepared for the grid dependency study. A steady-state solver, standard pressure interpolation scheme and SKE turbulence model were employed. Predicted temperature contour from the three different grid densities is shown in Fig. 3. The coarse grid under-resolved the temperature slightly, whereas the intermediate and fine grids offer much better resolution of the combustion process, as reflected in the predicted contour temperature. In the experimental work studied by Zain et al. [12], a type-k thermocouple was installed at the position of 5.85 m after the inlet position and 0.373 m from the PCL wall. The experimentally measured temperature was reported at 1293 K. The predicted temperature obtained from the three different grid densities were compared with the experimental data from our previous work [12]. Among the three different grids, the prediction using the coarse grid yielded the largest error (6.64%). A notable improvement in the prediction accuracy obtained using the intermediate (5.86%) and fine (5.68%) grids were observed. In terms of the computational time, prediction using higher grid density requires longer computing time. The CPU time spent by the coarse grid is below 0.9 s-iteration, whereas the intermediate and fine grids took about 1.8 and 2.7 s-iteration, respectively. Thus, the intermediate grid was selected for the remainder of this work to minimise the computational effort, since prediction by the fine and intermediate grids is not substantially different.

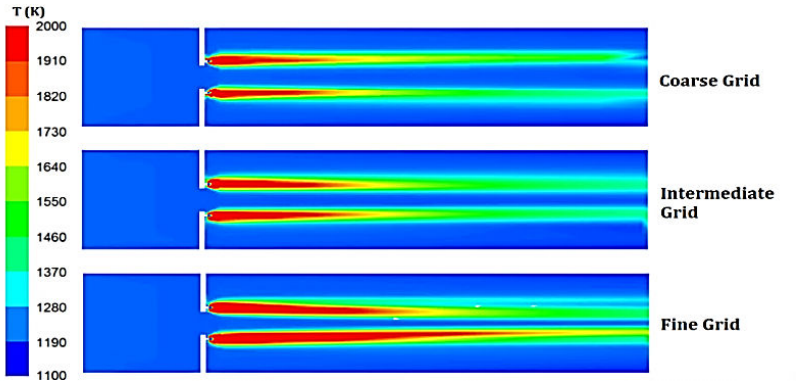


**Fig. 3. Temperature contour plot for three different grid densities.**

### 3.2. Discretisation

The effect of three different discretisation schemes (i.e., first-order upwind, second-order upwind and QUICK) on the CFD prediction were studied using a standard pressure interpolation scheme and SKE turbulence model. The comparison of the temperature predictions deviation to the experimental measurement [12] is shown in Fig. 4. The fastest convergence was achieved using the first-order upwind scheme. Nonetheless, the prediction is less accurate (7.49%) compared to the higher-order schemes due to the susceptibility of the first-order upwind scheme to the numerical diffusion. The higher-order schemes (i.e., second order and QUICK) have a better prediction than the first-order upwind scheme, but the difference is not remarkable, since both schemes show a similar error of 5.86%. Since the standard deviation obtained using the second-order upwind scheme is slightly lower than that achieved by the QUICK, hence second-order upwind scheme was used for the rest of this work.

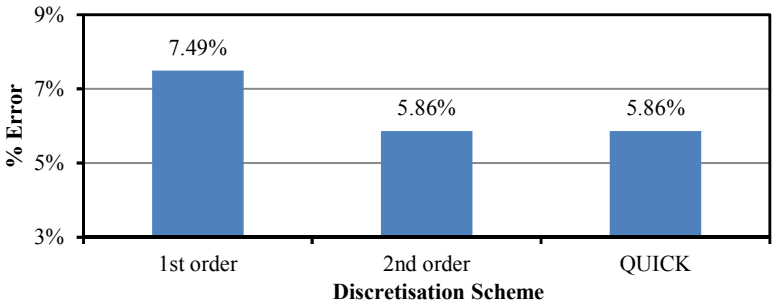


**Fig. 4. Comparison of discretisation scheme.**

### 3.3. Pressure interpolation scheme

The effect of the pressure interpolation scheme on the prediction accuracy of the temperature in the PCL was evaluated using a second-order upwind scheme and a SKE model. The four different pressure interpolation schemes are standard, second-order, linear and PRESTO (Pressure staggering option). Figure 5 shows the comparison of the temperature predictions obtained using four different pressure interpolation schemes with the experimental measurement [12]. The prediction accuracy achieved from these different pressure schemes is very close to each other, with error ranging from 5.86 to 6.03%. Among the four schemes, the standard pressure scheme obtained the lowest prediction error (5.86%), whereas the prediction using PRESTO showed the highest error (6.03%) and standard deviation. In fact, PRESTO is well suited for an unstable flow feature in the presence of high curvature and swirling flows, thus, this scheme may not perform well in a fairly simple flow in the PCL. Other pressure interpolation schemes showed the error below 6%. Theoretically, the prediction using the second-order pressure scheme should be more accurate than the linear pressure scheme. This is because the linear pressure scheme solves the face pressure as average pressure, whereas the second-order pressure scheme rebuilds the face pressure in the second-order accurate convection terms [21]. Results obtained in this work are also in agreement with this theory, although the difference between the second order and linear scheme is merely 0.03%. However, the standard

pressure scheme is reasonably accurate for the most cases and the other schemes are only considered when the standard pressure scheme is not applicable [21]. In this work, the standard pressure scheme is sufficient for the fluid flow modelling in a PCL.

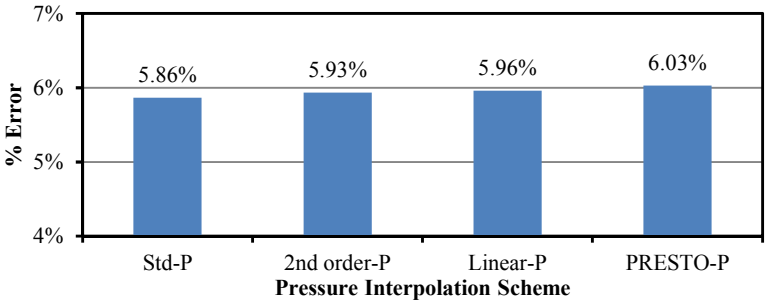


**Fig. 5. Comparison of pressure interpolation scheme.**

## 3.4. Turbulence model

The effects of various turbulence models (i.e., SKE, RKE and RNG) were studied using a steady-state simulation, the second-order upwind scheme and a standard pressure interpolation scheme. The results clearly showed that the SKE model yielded the lowest error (5.86%) compared to the other turbulence models. The RKE and RNG showed 7.04% and 6.82% error, respectively. This may be attributed by the fact that flow in a PCL is mostly homogeneous turbulence, which favours SKE. The fluid flow in a PCL as shown in Fig. 6 did not feature a strong curvature and swirling flow, which suited the RNG and RKE well [21, 22]. The minor disturbance by the oxygen lance did not affect the overall flow greatly. Nevertheless, all the turbulence models tested in this work can give a fair prediction of flow field in a PCL.

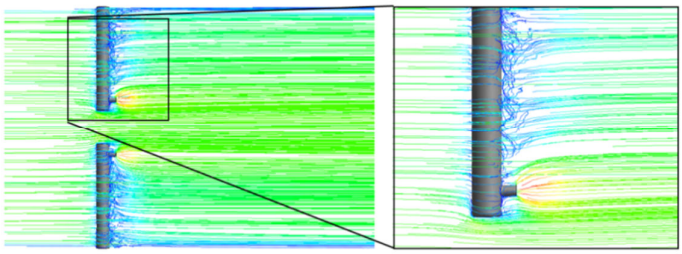

**Fig. 6. Streamline flow of a PCL.**

## 3.5. Effect of oxygen flowrate

The influence of the oxygen flowrate on the combustion temperature was studied by evaluating two different cases, i.e., dual lances operating at different flowrates; and single and dual lances operating at a similar total flowrate. The predicted temperature profile along the radial position at 5.85 m from PCL inlet is shown in Fig. 7. The dual temperature peak was observed at two regions (-0.3

m < Y < -0.1 m and 0.1 m < Y < 0.3 m) when dual lance is used. Whereas only a single temperature peak at -0.3 m < Y < -0.1 m was observed in the single lance operation. Higher oxygen flowrate enhanced the combustion reaction. This resulted in larger flame and higher temperature as shown in Fig. 8. Thereby, increasing the oxygen flowrate from 70 m/s to 100 m/s in dual lance operation increased the peak temperature from 1386 K to 1553 K (12% increased). The second case evaluates the effect of single and dual lance operating at a similar total flowrate. The two lances have a same surface area, in a way that the oxygen flowrate is proportional to the inlet velocity. The dual lance was set to operate at 70 m/s in each lance while the single lance was set to operate at 140 m/s to ensure a similar total flowrate can be obtained. A single lance produced higher temperature and wider flame in the combustion zone (Fig. 8). However, the combustion rate decreased towards the PCL outlet due to high consumption of fuel at the combustion zone. Therefore, the peak temperature achieved from a single lance (1328 K) is lower than the dual lance (1386 K).

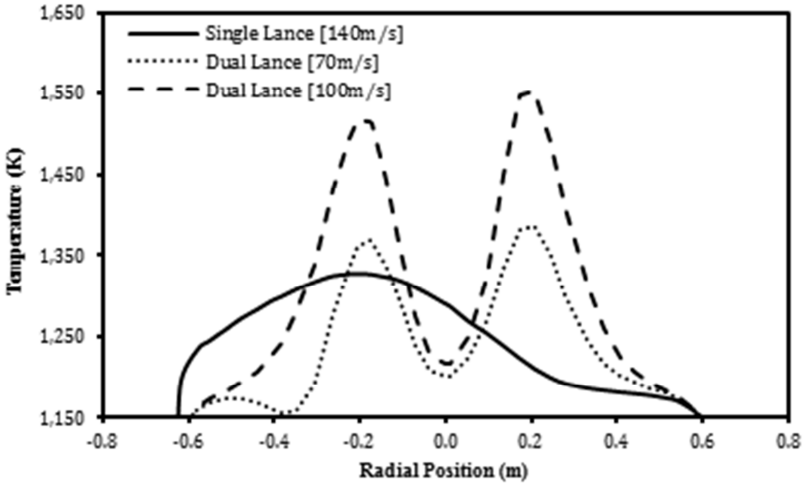


**Fig. 7. Predicted temperature profile for different oxygen flowrate.**

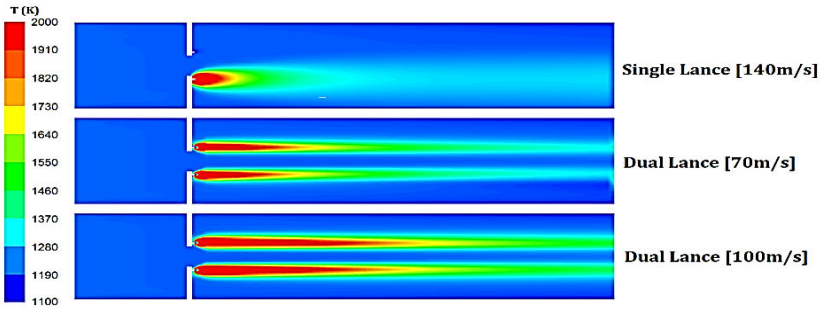


**Fig. 8. Temperature contour plot for different oxygen flowrate.**

## 4. Conclusions

A CFD modelling strategy was successfully developed for a three-dimensional PCL. From this study, we found that:

- A combination of a steady-state solver, SKE, second-order upwind and standard pressure interpolation scheme give a reasonably accurate prediction of the simultaneous heat transfer and reactive flow in the PCL.
- The CFD prediction showed a good agreement with the experimentally measured temperature with an error of 5.86%.
- It was found that a 40% increase in the oxygen flowrate yielded a 12% increased of combustion temperature.
- This work also indicated that dual lance provides a better combustion performance than the single lance working at same total oxygen flowrate.

## Acknowledgement

W.P. Law acknowledges to MyMaster scholarship from Ministry of Education Malaysia. The authors also acknowledge the research funding (GRS140331) from Universiti Malaysia Pahang.

## References

1. Saso, Y.; Gotoda, H.; and Ogawa, Y. (2005). Effect of oxygen concentration on the carbon monoxide yields from methane and methanol flames. *Fire Safety Science-Proceedings of the Eight International Symposium*, International Association for Fire Safety Science, 1013-1022.
2. Amirshaghaghi, H.; Zamaniyan, A.; Ebrahimi, H.; and Zarkesh, M. (2010). Numerical simulation of methane partial oxidation in the burner and combustion chamber of autothermal reformer. *Applied Mathematical Modelling*, 34, 2312-2322.
3. Li, G.; Zhou, H.; Qian, X.; and Cen, K. (2008). Determination of hydrogen production from rich filtration combustion with detailed kinetics based CFD method. *Chinese Journal of Chemical Engineering*, 16(2), 292-298.
4. Zhou, X.; Chen, C; and Wang, F. (2010). Modeling of non-catalytic partial oxidation of natural gas under conditions found in industrial reformers. *Chemical Engineering and Processing*, 49, 59-64.
5. Guo, W.; Wu, Y.; Dong, L.; Chen, C.; and Wang, F. (2012). Simulation of non-catalytic partial oxidation and scale-up of natural gas reformer. *Fuel Processing Technology*, 98, 45-50.
6. Bradley, D.; and Hundy, G.F. (1971). Burning velocities of methane-air mixtures using hot-wire anemometers in closed-vessel explosions. *Symposium (International) on Combustion*, 13(1), 575-583.
7. Zhang, Y.W.; Bo, Y.; Wu, Y.C.; Wu, X.C.; Huang, Z.Y.; Zhou, J.H.; and Cen, K.F. (2014). Flow behavior of high-temperature flue gas in the heat transfer chamber of a pilot-scale coal-water slurry combustion furnace. *Particuology*, 17, 114-124.

8. You, D.; Ham, F.; and Moin, P. (2008). Large-eddy simulation analysis of turbulent combustion in a gas turbine engine combustor. *Annual Research Briefs*, Center for Turbulence Research, 219-230.
9. Hassan, G.; Pourkashanian, M.; Ingham, D.; Ma, L.; and Taylor, S. (2009). Reduction in pollutants emissions from domestic boilers-computational fluid dynamics study. *Journal of Thermal Science and Engineering Applications*, 1, 1-9.
10. Galletti, C.; Parente, A.; and Tognotti, L. (2007). Numerical and experimental investigation of a mild combustion burner. *Combustion and Flame*, 151(4), 649-664.
11. Abbasi Khazaei, K.; Hamidi, A.A.; and Rahimi, M. (2010). CFD modeling study of high temperature and low oxygen content exhaust gases combustion furnace. *Iranian Journal of Chemistry & Chemical Engineering*, 29(2), 85-104.
12. Zain, M.I.S.; Gimbun, J.; and Hassan, Z. (2011). CFD study on the performance of oxygen lance for partial combustion unit at direct reduction plant. *Proceedings of the International Conference on Chemical Innovation 2011 (ICCI2011), ITC-TATIUC*, Teluk Kalong, Terengganu.
13. Shih, T.H.; Liou, W.W.; Shabbir, A.; Yang, Z.; and Zhu, J. (1994). A new *k-ε* eddy viscosity model for high Reynolds number turbulent flows: Model development and validation. *NASA technical memorandum 106721*, *ICOMP-94-21, CMOTT-94-6,* Lewis Research Center, Cleveland, Ohio.
14. Andersson, B.; Andersson, R.; Hakansson, L.; Mortensen, M.; Sudiyo, R.; and Wachem, B.V. (2012). *Computational Fluid Dynamics for Engineers*. Cambridge University Press, New York.
15. Yakhot, V.; and Orszag, S.A. (1986). Renormalization group analysis of turbulence. I. Basic theory. *Journal of Scientific Computing*, 1(1), 3-51.
16. Welty, J.R.; Wicks, C.E.; Wilson, R.E.; and Rorrer, G. (2001). *Fundamentals of Momentum, Heat, and Mass Transfe*r (4th Ed.). John Wiley & Sons, New York.
17. Gubba, J.; Ingham, D.B.; Larsen, K.J.; Ma, L.; Pourkashanian, M.; Tan, H.Z.; Williams, A.; Zhou, H. (2012). Numerical modelling of the co-firing of pulverized coal and straw in a 300MWe tangentially fired boiler. *Fuel Processing Technology*, 104, 181-188.
18. Keenan, J.H.; Chao, J.; Kaye, J. (1983). *Gas Tables*. John Wiley & Sons, New York.
19. Touloukian, Y.S.; Liley, P.E.; Saxena, S.C. (1975a). *Thermophysical Properties of Matter: Thermal Conductivity.* Vol. 3. IFI/Plenun, New York.
20. Touloukian, Y.S.; Saxena, S.C.; Hestermans, P. (1975b). *Thermophysical Properties of Matter: Viscosity.* Vol. 11. IFI/Plenun, New York.
21. Fluent Inc. (2006). *Fluent 6.3 user's guide*. Lebanon, NH.
22. Gimbun, J. (2008). CFD simulation of aerocyclone hydrodynamics and performance at extreme temperature. *Engineering Applications of Computational Fluid Mechanics*, 2(1), 22-29.